

Fully anisotropic superconducting transition in ion-irradiated $\text{YBa}_2\text{Cu}_3\text{O}_{7-\delta}$ with a tilted magnetic field

B. Espinosa-Arronte,^{1,*} M. Andersson,¹ C. J. van der Beek,² M. Nikolaou,³ J. Lidmar,³ and M. Wallin³

¹Department of Microelectronics and Applied Physics, KTH School of ICT, Royal Institute of Technology, SE-164 40 Kista, Sweden

²Laboratoire des Solides Irradiés, CNRS-UMR 7642 and CEA/DSM/DRECAM, Ecole Polytechnique, F-91128 Palaiseau, France

³Department of Theoretical Physics, KTH School of Engineering Sciences, Royal Institute of Technology, SE-106 91 Stockholm, Sweden

(Received 12 February 2007; published 21 March 2007)

We consider the superconducting vortex solid-to-liquid transition in heavy ion-irradiated untwinned $\text{YBa}_2\text{Cu}_3\text{O}_{7-\delta}$ single crystals in the case where the magnetic field direction does not coincide with that of the irradiation-induced linear columnar defects. For a certain range of angles, the resistivities measured in three orthogonal spatial directions vanish at the transition as three clearly different powers of reduced temperature. At previously known second-order phase transitions, scaling of physical quantities has either been isotropic or anisotropic in *one* direction. Thus, our findings yield evidence for a new type of critical behavior with *fully anisotropic* critical exponents.

DOI: 10.1103/PhysRevB.75.100504

PACS number(s): 74.72.Bk, 05.70.Fh, 74.25.Qt

Vortex matter in high temperature superconductors offers many opportunities to study the effects of disorder, fluctuations, and frustration, which lead to a variety of new phases and phase transitions.¹ Among these, the two principal thermodynamic phases are a dissipative vortex liquid at high temperatures, and a truly superconducting vortex solid at low temperatures. In clean superconductors, the vortex solid-to-liquid transition is a first-order melting transition. The presence of strong disorder is believed to turn it into a continuous isotropic “vortex glass” transition.² Then, many quantities develop power-law singularities upon approaching the transition, which define its critical exponents. The critical properties are insensitive to microscopic details such as small-scale anisotropies, and depend instead on such general features as symmetry and dimensionality, which determine the transition’s universality class. All phase transitions discovered so far are of two main types, those with isotropic scaling properties, and those with anisotropic scaling in one direction.

For point disorder the glass transition will be *isotropic*, i.e., the critical exponents are independent of direction, even though the material itself can be anisotropic, as is the case in, e.g., $\text{YBa}_2\text{Cu}_3\text{O}_{7-\delta}$ (YBCO). A markedly different situation occurs in superconductors containing linear columnar defects following irradiation by swift heavy ions.^{3–9} Such defects are very effective at pinning the vortex lines when a magnetic field is applied parallel to them; the vortex solid at low temperature is then a “Bose glass.”³ The columnar defects and the applied field both break the symmetry, making the Bose glass transition *anisotropic*, with different exponents parallel and perpendicular to the columns.³ An interesting situation occurs when the magnetic field is tilted away from the defects. For small tilt the vortices will stay on the columns, leading to a transverse Meissner effect. As the tilt angle or the temperature is increased the vortices will eventually depin and enter the vortex liquid phase. The transverse component of the magnetic field then makes all three directions nonequivalent and opens for the possibility of fully anisotropic scaling, i.e., with different critical exponents in all directions.¹⁰ Furthermore, the problem of vortex depinning

from columnar defects is formally equivalent to the Bose-glass transition of bosons in a random potential.³ In this analogy, the tilted magnetic field corresponds to an imaginary vector potential, resulting in a non-Hermitian localization problem.¹¹

Here, we investigate the vortex solid-to-liquid transition by electrical transport measurements performed in three orthogonal spatial directions on untwinned heavy-ion irradiated YBCO with the magnetic field tilted away from the columns. It appears that, for angles not too close to the principal crystal axes, the resistivity vanishes as a power law of reduced temperature with different exponents in the three directions. Thus, we provide experimental evidence for a phase transition with anisotropic critical exponents in all directions, thereby extending the possible type of universality classes.

YBCO single crystals were grown by a self-flux method in yttria stabilized zirconia crucibles.¹² As-grown untwinned crystals with typical sizes of $0.5 \times 0.2 \times 0.02 \text{ mm}^3$ were annealed at 400°C in flowing O_2 for a week. Such crystals show clear vortex melting signatures in magnetic fields. Irradiation with 1 GeV Pb^{56+} ions was performed at the Grand Accélérateur National d’Ions Lourds (GANIL), Caen, France, with the incident beam almost parallel to the crystallographic c axis. The resulting damage consists of randomly distributed amorphous tracks, with a diameter of about 7 nm, extending through the total thickness of the sample.¹³ Every ion impact creates a track. For most samples, the track density was $n_d = 1 \times 10^{11} \text{ ions cm}^{-2}$, corresponding to a matching field $B_\phi \equiv \phi_0/n_d = 2.0 \text{ T}$ ($\phi_0 = h/2e$ is the flux quantum). Electrical contacts were prepared by silver paint, giving contact resistances below 1.5Ω . For resistivity measurements in the x and y directions, perpendicular to the columns and parallel to the CuO_2 planes, the current pads were applied on opposite sides of the crystal. The resistivity parallel to the columns, ρ_z , was measured on another sample, with current contacts covering most of the ab -plane surfaces so as to assure the most homogeneous current distribution.¹⁴ The linear resistivity was measured using the standard four-probe technique, with a current of 0.1 mA and 1 mA for the in-plane

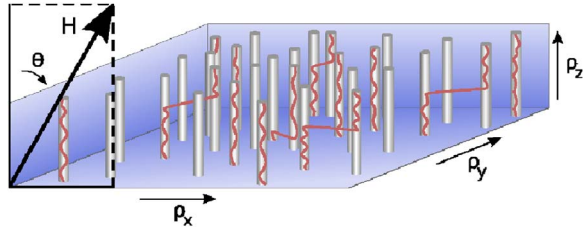


FIG. 1. (Color online) Experimental geometry. The columnar defects are parallel to the z direction, which coincides with the crystallographic c axis. The magnetic field is always applied in the xz plane, at an angle θ with respect to z . Vortex lines may accommodate the columns by forming kinks.

and c -axis measurements, respectively. Using a dc picovoltmeter as preamplifier, the voltage resolution was below 1 nV. The angular resolution of the field orientation is 0.01° along the direction of rotation of our single-axis rotating sample holder and 1° – 2° perpendicular to it.

The geometry of our experiment is shown in Fig. 1. The magnetic field, H , is always applied in the xz plane at an angle θ with respect to the direction of the columnar defects; $\rho_{x,y}$ were measured on the same sample mounted in different orientations with respect to the field direction. Figure 2 shows raw $\rho(T)$ data measured in the three spatial directions. The zero-field transition temperature for the crystal used for most of the ρ_x and ρ_y measurements was $T_{c0}=91.7$ K ($\Delta T_c \approx 0.5$ K); the crystal employed to measure ρ_z had $T_{c0}=91.2$ K ($\Delta T_c \approx 1$ K). The difference in T_{c0} accounts for the different vortex solid-to-liquid transition temperature T_c found in the ρ_z measurements. Our results are independent of the choice of x as either the crystallographic a or b axis.

Close to the vortex solid-to-liquid phase transition, the resistivity drops to zero as a power law of $|T/T_c - 1|$,

$$\rho_i = \rho_{0i} |T/T_c - 1|^{s_i}, \quad i = x, y, z. \quad (1)$$

From the measured $\rho_i(T)$ curves, s_i and T_c were determined in the standard way. A straight line was fit to the inverse logarithmic derivative of the experimental data $(\partial \ln \rho_i / \partial T)^{-1} = (T - T_c) / s_i$, as shown in Fig. 2. Below 5% of the normal state resistivity, power-law scaling corresponding to the critical regime is observed. All measurements are made in the linear response regime; therefore, the scaling is insensitive to circumstances such as possible nonlocality of vortex flow. We have also directly fitted the data to a power law (see Fig. 2), which yields consistent results.

The experimentally obtained exponents s_x , s_y , and s_z for $\mu_0 H = B_\phi$ are shown as a function of θ in Fig. 3(a). There are three distinct angular regimes, with different relations between the three exponents. For $\theta \leq 15^\circ$, $s_x \approx s_y$, while s_z is smaller. For $15^\circ \leq \theta \leq 65^\circ$ all s_i are different, with $s_y < s_x < s_z$. In this interval the best fits to the power law (1) were found. The exponents are approximately constant as a function of angle, suggesting a certain amount of universality. The average values $s_x = 4.9 \pm 0.2$, $s_y = 3.6 \pm 0.2$, and $s_z = 6.9 \pm 0.3$ are indicated by the dashed lines in Fig. 3(a). Finally, at angles above 65° , s_z decreases while s_x increases.

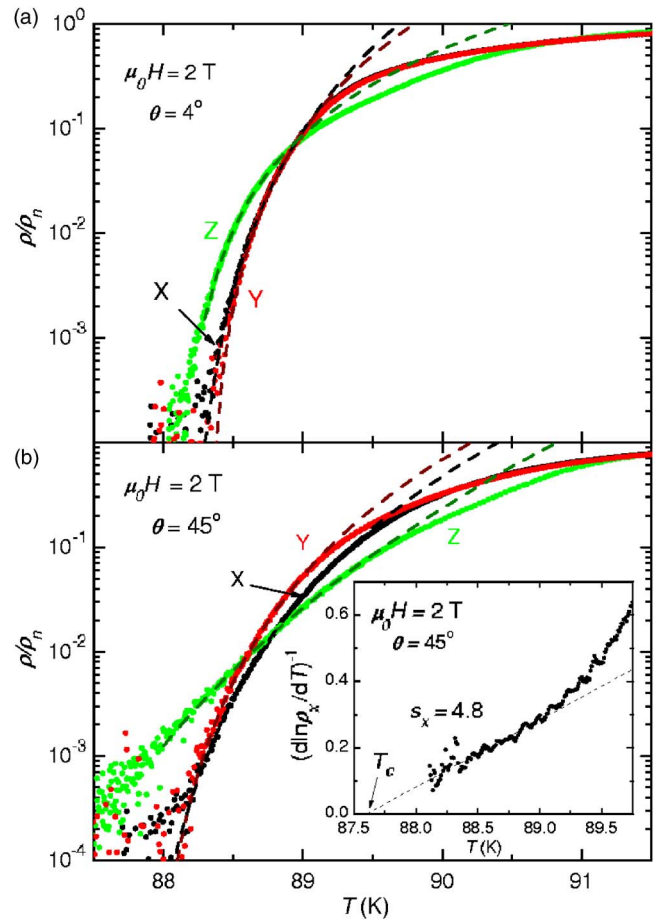


FIG. 2. (Color online) Normalized resistivity in three independent directions of an untwinned heavy-ion irradiated YBCO single crystal with a matching field $B_\phi = 2$ T, and at tilt angles (a) $\theta = 4^\circ$ and (b) $\theta = 45^\circ$ from the columns. Dashed lines are fits to Eq. (1). Inset: Extraction of T_c and the critical exponent s_i using $(\partial \ln \rho_i / \partial T)^{-1} = (T - T_c) / s_i$.

The error bars were estimated by varying the resistance interval of the fits while maintaining good agreement with the data.

The interaction between the columns and the vortices changes with tilt angle, which can explain the existence of several angular regimes with different behavior of the exponents. At angles below $\theta_L \approx 1^\circ$ – 2° ,¹⁵ the vortices are locked within the columns in the Bose-glass phase and a transverse Meissner effect is expected.^{3,15} The proximity to this phase will influence the transition and may explain the variation in the exponents for $\theta < 5^\circ$.¹⁵ For $\theta > \theta_L$, vortices adjust to the columnar defects by forming a staircase structure,^{1,3} depicted in Fig. 1. This occurs up to a certain accommodation angle θ_a determined by the balance between the pinning energy gained by the segments trapped on a column and the energy loss due to vortex line tilt. For $\theta > \theta_a$, the columns are thought to act as translationally symmetric “point pins.” The vortex lines intersect the columns only over a length corresponding to the vortex core radius, and are on average parallel to the direction of the applied field. Experimentally, θ_a is usually defined as the maximum of the angular-dependent resistivity,^{16,17} as shown in the inset of Fig. 4. In our experi-

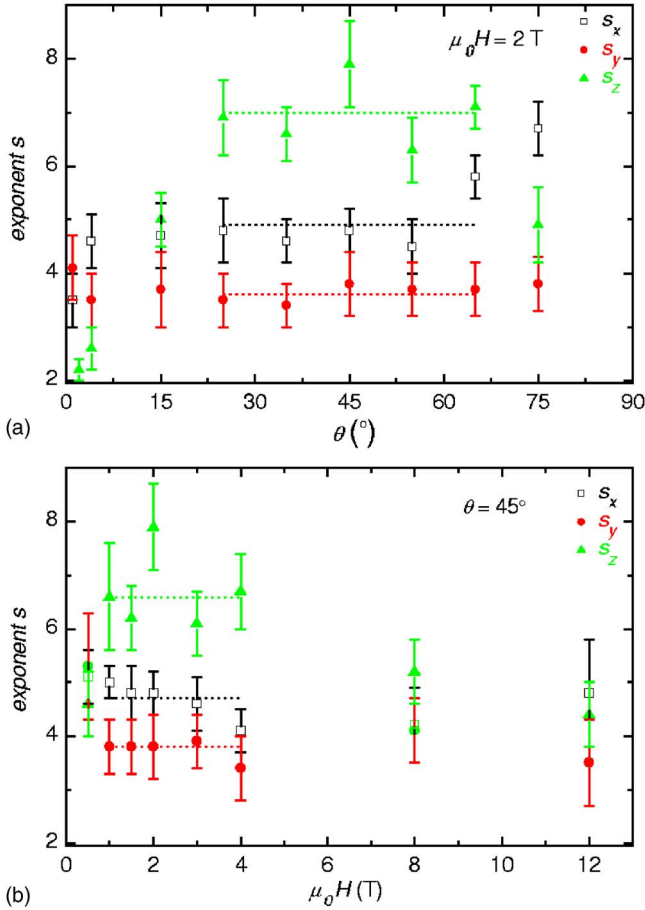


FIG. 3. (Color online) Exponents s_x , s_y , and s_z of the power-law Eq. (1) by which the resistivity vanishes at the vortex solid-to-liquid transition in the x , y , and z directions, respectively. (a) Exponents at 2 T as a function of angle θ . For $15^\circ \leq \theta \leq 65^\circ$, the scaling behavior is anisotropic in three directions. (b) Exponents at $\theta = 45^\circ$, as a function of magnetic field. There is anisotropic scaling at fields close to the matching field, $\mu_0 H \approx B_\phi = 2$ T. Dotted lines show the average value of s_i in the regimes of anisotropic scaling. The error bars are estimated from the quality of the fits in Fig. 2.

ments this gives $\theta_a \approx 15^\circ - 20^\circ$, which coincides with the observed change in the behavior of the critical exponents. However, it is *above* this so defined θ_a that three different resistivity exponents are observed. This suggests that the columnar defects still play a determining role in this regime, as they break the symmetry sufficiently strongly for the anisotropic scaling to be observed. Finally, as the field orientation perpendicular to the columns is approached, another change in the sequence of the exponents is observed, probably due to the layered nature of YBCO.¹⁸

Figure 3(b) shows that the values of s_i change as a function of H , indicating a change in the nature of the phase transition. At high fields, the vortex density exceeds the defect density. Hence, vortex-vortex interactions become increasingly important compared to the vortex-defect interaction, and the anisotropy of the transition described above should progressively disappear. Above 4 T, the exponents are roughly the same in all directions and more or less field independent. The difference between the exponents is most

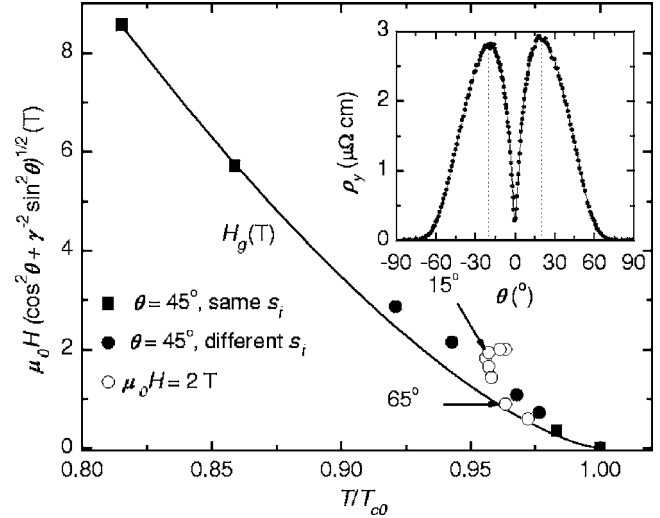


FIG. 4. Phase diagram for untwinned heavy-ion irradiated YBCO single crystals. An effective magnetic field is used to account for the anisotropy of YBCO. The symbols show the vortex solid-to-liquid transition temperatures obtained from measurements of ρ_y at constant $\theta = 45^\circ$ and several fields (■, ●); and at constant $\mu_0 H = 2$ T and different θ (○). At fields far from $B_\phi = 2$ T, isotropic glass exponents are found (■) and the data can be fitted to Eq. (2) (solid line). For fields comparable to B_ϕ the transition lies above this line. At $\theta \approx 15^\circ$ the transition bends toward the isotropic glass line; nevertheless, it remains above it up to $\theta \sim 65^\circ$. Inset, $\rho_y(\theta)$ at 1 T and 90.2 K. At $\theta = 0$ the field is aligned with the columns. The accommodation angle θ_a is usually defined by the maximum of $\rho(\theta)$ (dashed lines).

pronounced close to the matching field. The average values in this region are $s_x = 4.7 \pm 0.2$, $s_y = 3.8 \pm 0.2$, and $s_z = 6.6 \pm 0.3$, consistent with the average values at constant $\mu_0 H = 2$ T found above. At lower fields, the exponents again approach a common value. We observe these trends systematically irrespective of sample or matching field.

For high fields the effect of the columns is less relevant. Most vortices are pinned by pointlike pinning centers, or by the interaction with the “matrix” of vortices trapped on a column.¹⁹ The vortex solid resembles an isotropic glass, with identical power-law exponents in all directions. Then, the glass line is given by²⁰

$$H_g(T) \propto (1 - T/T_{c0})^n, \quad (2)$$

where T_{c0} is the zero-field transition temperature and $H_g = H[T = T_c(H)]$. Figure 4 shows the experimentally obtained solid-to-liquid transition temperatures $T_c(H)$ obtained from ρ_y . To account for the intrinsic anisotropy of YBCO an effective field $H_{\text{eff}} = H \sqrt{\gamma^{-2} \sin^2 \theta + \cos^2 \theta}$ is plotted on the ordinate ($\gamma \approx 7$ is the anisotropy parameter²¹). The figure also shows a fit to Eq. (2) of the T_c data at fields where approximately isotropic exponents s_i were found. The fit gives $n \approx 1.5$, in agreement with the value reported for the isotropic vortex glass.²⁰ We observe that for fields close to the matching field, and angles $\theta \leq 65^\circ$, $T_c(H)$ lies above the glass line (2). A bend toward this line is observed at an angle consistent with the experimentally defined $\theta_a \approx 15^\circ$ but, up to $\theta \sim 65^\circ$,

the data still lie above the $H_g(T)$ line. In fact, $T_c(H)$ resembles the behavior expected for the Bose-glass line,^{1,22,23} adding further evidence that the effect of the columns as correlated pinning centers is important even at angles *above* the experimentally defined θ_a .

We now discuss the value of the exponents in the field ($B \approx B_\phi$) and angular regime ($15^\circ < \theta < 65^\circ$) in which fully anisotropic scaling is observed. We assume that the anisotropic scaling is due to the different correlation length exponents in the three directions. Then, $\xi_x \sim \xi^\chi$, $\xi_y \sim \xi$, and $\xi_z \sim \xi^\zeta$, where $\xi \sim |T - T_c|^{-\nu}$. We also assume dynamic scaling for critical slowing down, described by the correlation time $\tau \sim \xi^z$, where z is the dynamic critical exponent. Following the procedure outlined in Ref. 10, the longitudinal resistivities are $\rho_i = \frac{E_i}{J_i} \sim (T - T_c)^{s_i}$, where $s_x = \nu(z - 1 + \chi - \zeta)$, $s_y = \nu(z + 1 - \chi - \zeta)$, and $s_z = \nu(z - 1 - \chi + \zeta)$. Thus, the observation of three different s_i 's suggests that the correlation length diverges with different exponents in all directions. An additional constraint is needed for extracting ν , χ , and ζ from the experiments. Given the similarity between the Bose glass and the transverse Meissner transitions¹⁰ on the one hand and the transition observed here on the other, one may argue that the relation $\zeta - \chi - 1 = 0$, which follows if the compressibility remains finite at the transition, should remain valid. If this is

so, the experimentally observed s_i yield $\nu = 1.0 \pm 0.4$, $\chi = 1.6 \pm 0.7$, $\zeta = 2.6 \pm 0.7$, and $z = 6.9 \pm 2.2$. This can be compared with the results on the transverse Meissner transition ($\nu \approx 0.70$, $\chi = 2$, and $\zeta = 3$), indicating that the transition observed here may be of somewhat different nature.

In summary, for certain angles between the field and the columns and at vortex densities close to the defect density, the resistivity of heavy-ion irradiated untwinned YBCO vanishes as a power law of reduced temperature with different exponents in all three directions. This shows that the scaling properties of the phase transition are fully anisotropic in three dimensions. Thus, our findings provide experimental evidence for a new kind of universal scaling behavior at a second-order phase transition. It would be of interest to search for anisotropic scaling behavior in other physical systems with a similar symmetry breaking as the one considered here.

The authors thank M. Konczykowski for his presence during the irradiation and Ö. Rapp for valuable comments. This work has been supported by the Swedish Research Council (Vetenskapsrådet) and the Swedish Foundation for Strategic Research through the OXIDE program. The Göran Gustafsson Foundation is acknowledged for supporting the work of one of the authors (M.N.) and financing equipment.

*Electronic address: beatriz@kth.se

¹G. Blatter, M. V. Feigel'man, V. B. Geshkenbein, A. I. Larkin, and V. M. Vinokur, *Rev. Mod. Phys.* **66**, 1125 (1994).

²D. S. Fisher, M. P. A. Fisher, and D. A. Huse, *Phys. Rev. B* **43**, 130 (1991).

³D. R. Nelson and V. M. Vinokur, *Phys. Rev. Lett.* **68**, 2398 (1992); *Phys. Rev. B* **48**, 13060 (1993).

⁴D. R. Nelson and L. Radzihovsky, *Phys. Rev. B* **54**, R6845 (1996).

⁵J. Lidmar and M. Wallin, *Europhys. Lett.* **47**, 494 (1999).

⁶W. Jiang, N.-C. Yeh, D. S. Reed, U. Kriplani, D. A. Beam, M. Konczykowski, T. A. Tombrello, and F. Holtzberg, *Phys. Rev. Lett.* **72**, 550 (1994).

⁷S. A. Grigera, E. Morr e, E. Osquiguil, C. Balseiro, G. Nieva, and F. de la Cruz, *Phys. Rev. Lett.* **81**, 2348 (1998).

⁸D. S. Reed, N. C. Yeh, M. Konczykowski, A. V. Samoilov, and F. Holtzberg, *Phys. Rev. B* **51**, 16448 (1995).

⁹R. J. Olsson, W. K. Kwok, L. M. Paulius, A. M. Petrean, D. J. Hofman, and G. W. Crabtree, *Phys. Rev. B* **65**, 104520 (2002).

¹⁰A. Vestergren, J. Lidmar, and M. Wallin, *Phys. Rev. Lett.* **94**, 087002 (2005).

¹¹N. Hatano and D. R. Nelson, *Phys. Rev. Lett.* **77**, 570 (1996).

¹²Y. Eltsev, W. Holm, and Ö. Rapp, *Phys. Rev. B* **49**, 12333 (1994).

¹³Y. Yan and M. A. Kirk, *Phys. Rev. B* **57**, 6152 (1998).

¹⁴B. Lundqvist, Ö. Rapp, M. Andersson, and Y. Eltsev, *Phys. Rev. B* **64**, 060503(R) (2001).

¹⁵A. W. Smith, H. M. Jaeger, T. F. Rosenbaum, A. M. Petrean, W. K. Kwok, and G. W. Crabtree, *Phys. Rev. Lett.* **84**, 4974 (2000).

¹⁶R. C. Budhani, W. L. Holstein, and M. Suenaga, *Phys. Rev. Lett.* **72**, 566 (1994).

¹⁷A. Pomar, L. Martel, Z. Z. Li, and H. Raffy, *Phys. Rev. B* **63**, 134525 (2001).

¹⁸W. K. Kwok, J. Fendrich, U. Welp, S. Fleshler, J. Downey, and G. W. Crabtree, *Phys. Rev. Lett.* **72**, 1088 (1994).

¹⁹M. Menghini, Y. Fasano, F. de la Cruz, S. S. Banerjee, Y. Myasoedov, E. Zeldov, C. J. van der Beek, M. Konczykowski, and T. Tamegai, *Phys. Rev. Lett.* **90**, 147001 (2003).

²⁰T. Klein, A. Conde-Gallardo, J. Marcus, C. Escribe-Filippini, P. Samuely, P. Szabo, and A. G. M. Jansen, *Phys. Rev. B* **58**, 12411 (1998).

²¹G. Blatter, V. B. Geshkenbein, and A. I. Larkin, *Phys. Rev. Lett.* **68**, 875 (1992).

²²L. Krusin-Elbaum, L. Civale, G. Blatter, A. D. Marwick, F. Holtzberg, and C. Feild, *Phys. Rev. Lett.* **72**, 1914 (1994).

²³A. I. Larkin and V. M. Vinokur, *Phys. Rev. Lett.* **75**, 4666 (1995).